Cytokine 169 (2023) 156296

Contents lists available at ScienceDirect

Cytokine

journal homepage: www.elsevier.com/locate/cytokine

Predicting cytokine kinetics during sepsis; a modelling framework from a porcine sepsis model with live *Escherichia coli*

Salma M. Bahnasawy [a], Paul Skorup [b], Katja Hanslin [c], Miklós Lipcsey [d], Lena E. Friberg [a], Elisabet I. Nielsen [a,*]

[a] Department of Pharmacy, Uppsala University, Uppsala, Sweden
[b] Section of Infectious Diseases, Department of Medical Sciences, Uppsala University, Uppsala, Sweden
[c] Anesthesiology and Intensive Care, Department of Surgical Sciences, Uppsala University, Uppsala, Sweden
[d] Hedenstierna laboratory, Anesthesiology & Intensive Care, Department of Surgical Sciences, Uppsala University, Uppsala, Sweden

ARTICLE INFO

Keywords:
Sepsis
IL-6
TNF
Non-linear mixed effect modelling

ABSTRACT

Background: Describing the kinetics of cytokines involved as biomarkers of sepsis progression could help to optimise interventions in septic patients. This work aimed to quantitively characterise the cytokine kinetics upon exposure to live *E. coli* by developing an *in silico* model, and to explore predicted cytokine kinetics at different bacterial exposure scenarios.

Methods: Data from published *in vivo* studies using a porcine sepsis model were analysed. A model describing the time courses of bacterial dynamics, endotoxin (ETX) release, and the kinetics of TNF and IL-6 was developed. The model structure was extended from a published model that quantifies the ETX-cytokines relationship. An external model evaluation was conducted by applying the model to literature data. Model simulations were performed to explore the sensitivity of the host response towards differences in the input rate of bacteria, while keeping the total bacterial burden constant.

Results: The analysis included 645 observations from 30 animals. The blood bacterial count was well described by a one-compartment model with linear elimination. A scaling factor was estimated to quantify the ETX release by bacteria. The model successfully described the profiles of TNF, and IL-6 without a need to modify the ETX-cytokines model structure. The kinetics of TNF, and IL-6 in the external datasets were well predicted. According to the simulations, the ETX tolerance development results in that low initial input rates of bacteria trigger the lowest cytokine release.

Conclusion: The model quantitively described and predicted the cytokine kinetics triggered by *E. coli* exposure. The host response was found to be sensitive to the bacterial exposure rate given the same total bacterial burden.

1. Introduction

Bacterial infections trigger a potent host immune response, that needs to be well-regulated to be sufficient for infection eradication without causing self-harm [1]. Sepsis, a life-threatening condition, occurs when a dysregulated host immune response to infection develops. This triggers a generalised systemic immune response exceeding the response required for a local infection clearance ultimately leading to multiple organ dysfunction [2]. A key feature of sepsis is the imbalance between the pro-inflammatory and anti-inflammatory components of the typical immune response [3]. The latest estimate points to that almost 20% of total deaths worldwide every year are attributed to sepsis [4]. In 2017, the World health organisation (WHO) recognised sepsis as a global health priority by adopting a resolution to improve, prevent, diagnose, and manage sepsis [5].

The innate immune response activation plays a fundamental part in the pathogenesis of sepsis. This is mediated by the recognition of unique pathogen-associated molecular patterns (PAMPs) like endotoxin (ETX), a Gram-negative bacteria outer membrane component. When ETX is recognised by Toll-like receptor-4 (TLR-4), a downstream molecular cascade is provoked leading to the release of cytokines, and other inflammatory regulators [2]. Cytokines are inflammatory mediators that play a crucial role in the pathophysiology of sepsis. Under normal physiologic condition, they regulate the activation and migration of

* Corresponding author at: Department of Pharmacy, Uppsala university, Box 580, 75123 Uppsala, Sweden.
E-mail address: elisabet.nielsen@farmaci.uu.se (E.I. Nielsen).

https://doi.org/10.1016/j.cyto.2023.156296
Received 11 May 2023; Received in revised form 23 June 2023; Accepted 5 July 2023
Available online 17 July 2023

immune cells to the site of infection, helping to clear the infection. In sepsis, a malfunctional cytokine network with tremendous release of cytokines (referred to as a cytokine storm) provokes a systemic response leading to endothelial dysfunction, coagulopathy, and tissue damage [6]. Examples of prominent cytokines that markedly signify sepsis progression include proinflammatory cytokines like tumour necrosis factor (TNF), and interleukin-6 (IL-6) [3,7]. The intricate interplay between the inflammatory and immunosuppressive phases of sepsis is highly dynamic, and they are usually overlapping without a clear temporal margin separating them [8].

Selecting appropriate therapy in sepsis is challenging. The profound pathophysiologic alterations occurring in sepsis result in high variability in the pharmacokinetics of administered medications [9]. Further, attempts to use immunomodulators in sepsis are hampered by the need to identify the type of intervention (i.e. immunostimulatory/immunosuppressive) required by each patient at a given point in the disease course [10]. Hence, describing the kinetics of different cytokines involved as potential biomarkers of sepsis progression could help to optimise medical interventions in septic patients [11].

Large animal models, like the porcine model, provides potential for translational research in sepsis. In a recent review on the challenges of translational research in sepsis, Cavaillon *et al.* identified an inappropriate animal model (e.g. mice) as one factor contributing to translational research failure [12]. Dissimilarities in the immune system and physiology, along with ETX resistance may explain the poor proxy of mice models for the human responses in sepsis. The immune system in pigs closely resembles humans with about 80% shared immune machinery, unlike the mice which shows less than 10% similarity [13]. Moreover, unlike mice, pigs have greater sensitivity to infection and their large size allows close monitoring of vital signs. Furthermore, several recent examples highlights the potential of applying mathematical modelling to increase the understanding of the complex and dynamic host-pathogen interaction in translational immunology research [14–16].

Mathematical modelling is a potential tool to evaluate the interplay of the host-pathogen interaction [14]. It provides a deeper insight into the time courses of the different components of this interaction. Recently, a non-linear mixed effect model was developed based on data on porcine endotoxemia in anesthetised piglets receiving ETX infusion [16]. This modelling approach allows data from different studies to be analysed simultaneously, while capturing the population mean parameters, and different sources of variabilities [17]. The model characterises the pro-inflammatory component of the host immune response by quantifying the kinetics of TNF and IL-6, as well as the temporal aspects of ETX tolerance development.

Although ETX plays a crucial role in sepsis pathogenesis, the clinical relevance of using experimental endotoxemia as a model for sepsis is debated [18–19]. It has been argued that the use of ETX as the only PAMP ignores the possible contribution of other bacterial components in the study of the host-pathogen interaction [20]. However, there is still limited knowledge whether the immune response would be different if triggered by exposure to the intact live bacteria rather than ETX only [1,21].

The overarching goal of the current work was to quantitively characterise the cytokine kinetics triggered by exposure to intact live Gram-negative bacteria during sepsis. The specific aims were to; (i) expand the previous model to describe the dynamics of *Escherichia coli (E. coli)in vivo* and the associated release of ETX, (ii) link the bacterial kinetics to the previously developed ETX-cytokines model and evaluate the need to refine the model, (iii) evaluate the model performance by applying the model to external data from the literature, and (iv) use the model to explore the cytokine kinetics at different bacterial exposure scenarios.

2. Methods

2.1. Data and study design

The current analysis included data from three previously published *in vivo* studies using a porcine sepsis model [22–24]. In each study, Swedish landrace pigs (22.4–33.1 kg) received a three-hour continuous infusion of live *E. coli* strain B09-11822 (serotype O rough:K1:H7; Statens Seruminstitut, Copenhagen, Denmark) succeeded by a follow-up period of three hours. Blood samples were collected for measurements at 1, 2, 3 h from the start of infusion for blood bacterial count, 0, 2, 4, 6 h for ETX, and 0, 1, 2, 3, 4, 5, 6 h for both TNF and IL-6. The total administered dose of bacteria was 5×10^8 CFU, with accepted range $3.5–7.1 \times 10^8$ CFU. A fresh bacterial infusate was prepared hourly to ensure the bacteria being in the logarithmic phase of growth. The piglets received the bacteria through a central vein catheter, except for one study [22] where they received the infusions through the portal vein preceded by a 24-hour saline infusion. The data obtained from the different studies were treated similarly given the lack of significant discrepancies in the time courses of the measured samples. Exploratory plots for the data from the different studies is provided in Fig. 1s in the supporting information file. Anaesthesia and ventilation protocols were the same across studies and have been described previously [22–24]. The animals included in the current analysis did not receive any antibiotic treatment throughout the study.

2.2. Model development

A model describing the time courses of bacterial dynamics, ETX release, and the induced changes of the two cytokines TNF and IL-6 was developed. The model structure from Thorsted *et al.* [16] was extended to include additional compartments describing the kinetics of *E. coli* and the associated release of ETX and linked to the previously developed ETX-cytokines model.

The four dependent variables (DVs); bacterial count, ETX, TNF and IL-6, were sequentially considered for model fitting. Different structural models were tested for describing bacterial dynamics and the associated ETX release (e.g. a 1 or 2-compartment model, with or without bacterial multiplication, with linear or non-linear elimination). Thorsted's structural model was applied to the cytokines data while first fixing the model parameters. Thereafter, the parameters from Thorsted's model were allowed to be re-estimated for the new data by using informed priors. Linear stimulatory effect of bacteria was tested on TNF production with and without exponential time decay function to explore the possible contribution of bacteria on stimulating TNF production.

Priors were implemented by using NONMEM PRIOR functionality with NWPRI subroutine. This approach of using frequentist priors help to stabilise the estimation of model parameters and reduce the bias given the possibility of parameter differences in the current study population. In this context, a penalty function for the priors derived from a normal-inverse Wishart distribution is considered during objective function estimation. The informativeness (i.e. weight) of prior parameters to the model would depend on parameter uncertainty for fixed-effect parameters and on the degree of freedom for random-effect parameters (ω) [25]. The variance–covariance matrix of the parameter estimates in Thorsted's model was used to define the uncertainty and the degree of freedom was calculated based on the formula;

$$\mathrm{df} = 2 \cdot \left(\frac{\omega^2}{\mathrm{SE}(\omega^2)} \right)^2 + 1 \quad (1)$$

where ω^2 is the variance estimate of the previous analysis, and $SE\left(\omega^2\right)$ is the reported standard error.

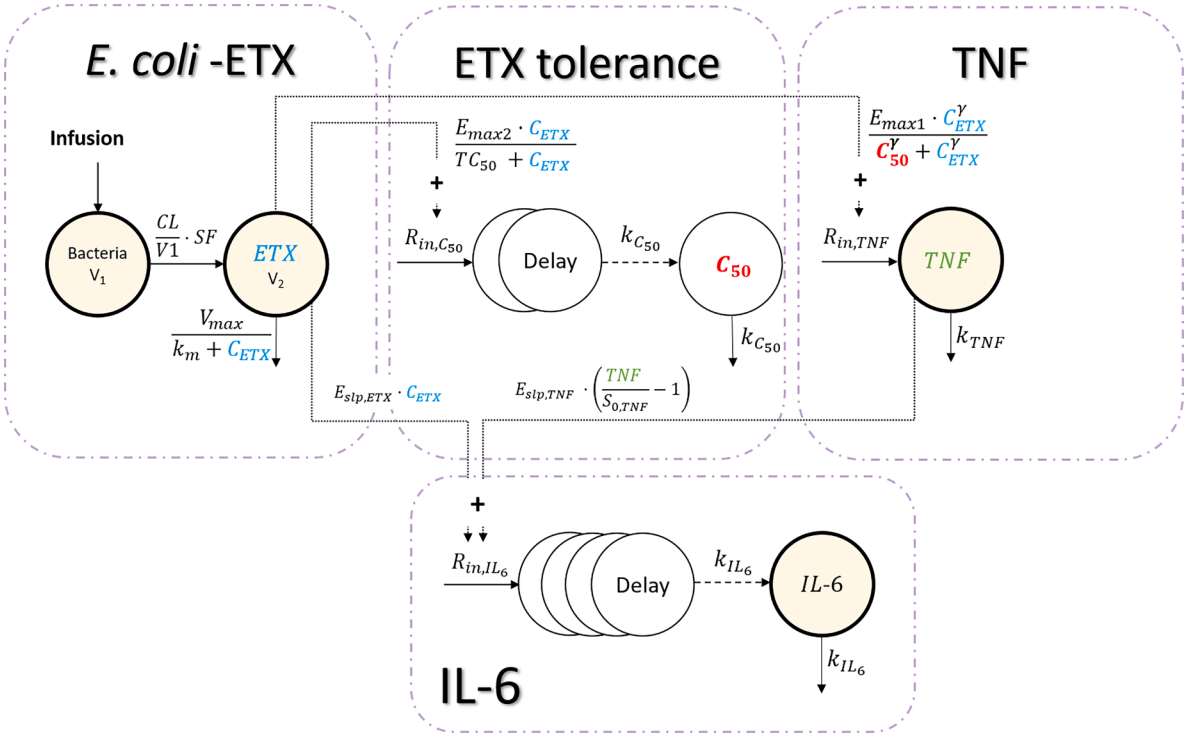

Fig. 1. Model schematic. Yellow coloured circles indicate observed variables, dotted lines indicate stimulatory functions, and dashed lines indicate transit compartment delays. Coloured text is used to highlight the variables that drive downstream equations. Parameter descriptions are supplied in Table 2.

2.3. Modelling framework and software

Model estimation was performed using a nonlinear mixed-effects model framework in NONMEM version 7.5 (ICON Development Solutions, Ellicott City, MD, United States). Model runs were executed using Perl-Speaks-NONMEM 5.2.6 (PsN), Pirana 2.9.9. Data handling and post processing of estimation runs including model diagnostics were performed in R using and xpose4, and tidyverse packages.

Model selection was based on the reduction in the objective functions value (OFV) using the likelihood ratio test for nested models at a predefined P-value less than 0.05. The precision of parameter estimates, and goodness of fit plots were also considered for model selection. For the parameters that were informed by priors, the ratio of relative standard error (RSE) of the updated estimates of the final model and prior estimate from previous population was calculated to evaluate informativeness of priors. Model performance was evaluated based on the visual inspection of individual plots, and prediction corrected visual predictive checks (pcVPCs) [26].

For each variable, both the observed data and model predictions were log transformed and additive residual error models on the log-scale were used (equivalent to proportional error models on untransformed data). Exponential models were adopted to describe the between-subject variability. Importance sampling (IMP) with interaction was used for model fitting. Observations below the limit of quantification (BLOQ) were treated as censored data, with maximization of the likelihood of these data being BLOQ [27]. For TNF, only one observation (0.5% of the data) was BLOQ, and hence, this observation was omitted.

2.4. Model external evaluation

External model evaluation was performed using data extracted from the literature where a similar porcine sepsis model had been used. The data arose from three studies [28–30] (n = 12;8;8) where piglets received a four-hour continuous intravenous infusion of live *E. coli* (strain LE392-ATCC 33572) with dose up-titration. Measurements of TNF, and IL-6 were reported as mean observations at 0, 0.5, 1, 2, 3, 4 hours. A summary of the main differences in the study design of the external data and the current analysis data is provided in Table 1.

The data points were digitised using WebPlotDigitizer [31]. The model simulations were performed in R using RxODE package. TNF, IL-6 profiles were predicted over four hours at the reported escalated infusion rate. The model predictions were overlaid on the digitised observed data (reported as means ± SEM or 95% confidence interval). For the data points where SEM was reported, 95% CI was derived assuming normal distribution.

2.5. Model simulations for different bacterial exposure scenarios

The model was used to simulate the cytokine kinetics that could develop at different exposure scenarios to the bacteria. The aim of these simulations was to explore the sensitivity of the host response to the bacterial exposure profile (e.g. increasing, decreasing, or constant prolonged bacterial exposure) given the same total bacterial burden. In

Table 1
Study design aspects for the present [19–21] and external data [25–27].

	Present data	External data
Study population	Swedish landrace pigs (25–35 kg) (n = 30)	Norwegian landrace pigs (13–17 kg) (n = 12, 8, 8)
Bactetrial strain	Live *E. coli* (strain B09-11822)	Live *E. coli* (strain LE392-ATCC 33572)
Infusion rate	3- hour infusion, constant infusion rate (fresh infusate replaced hourly) 1.67×10^8 CFU/h	4- hour infusion, with dose up-titration 3.75×10^7 CFU/h (0 → 1 h) 1.5×10^8 CFU/h (1 → 1.5 h) 6.0×10^8 CFU/h (1.5 → 4 h)
Total bacterial challenge dose	Total dose 5×10^8 CFU	Total dose 1.075×10^8 CFU/kg ≈ 16×10^8 CFU
Analysis kit for cytokines	DuoSet® porcine immunoassay kits from R&D Systems (Minneapolis, MN).	Quantikine® porcine immunoassay kits from R&D Systems (Minneapolis, MN).

these simulations, the total bacterial burden was fixed to 5×10^8 CFU received as continuous infusion, with different infusion scenarios;

(i) Three-hour infusion with constant infusion rate of 1.67 CFU $\times$ $10^8 h^{-1}$
(ii) Six-hour infusion with constant infusion rate of 0.83 CFU $\times$ $10^8 h^{-1}$
(iii) Three-hour infusion with dose up-titration every hour for two scenarios;
  (a) 0.25, 0.75, then 4.0 CFU $\times$ $10^8 h^{-1}$; corresponding to 5%, 15%, 80% of total dose
  (b) 1.0, 1.5, then 2.5 CFU $\times$ $10^8 h^{-1}$; corresponding to 20%, 30%, 50% of total dose
(iv) Three-hour infusion with dose down-titration every hour for two scenarios;
  (a) 2.5, 1.5, then 1.0 CFU $\times$ $10^8 h^{-1}$; corresponding to 50%, 30%, 20% of total dose
  (b) 4.0, 0.75, then 0.25 CFU $\times$ $10^8 h^{-1}$; corresponding to 80%, 15%, 5% of total dose

3. Results

3.1. Model structure

A schematic of the final model structure is depicted in Fig. 1. The model described the time courses of bacterial count, ETX, TNF and IL-6 (code provided in the supporting information file). The analysis included data from 30 animals with a total of 645 observations (bacterial count (n = 133), ETX (n = 79), TNF (n = 214) and IL-6 (n = 219)). A summary of the number of samples and the lower limit of quantification (LLOQ) of measured variables from the different studies is supplied in Table 1s in the supporting information file.

3.1.1. Bacterial dynamics and ETX release

The blood bacterial count was well-described by a one-compartment distribution model with linear elimination according to;

$$\frac{d(B)}{dt} = -\frac{CL}{V_1} \cdot B \quad ; \; B_0 = 0 \tag{2}$$

where B is the blood bacterial count in CFU, CL is bacterial clearance, V_1 is the bacteria volume of distribution, and B_0 the initial blood bacterial burden.

Adding a bacterial growth rate constant did not improve the model fit as reflected by the lack of statistically significant drop in the objective functions value (Δ OFV = -0.145 vs. model without bacterial growth). Further, a two-compartment model for bacterial distribution failed to show a statistically significant improvement (ΔOFV = -0.041 vs. one-compartment model), and an estimation of non-linear elimination was not supported by the current data (did not converge successfully).

Allometric scaling by body weight was implemented on CL and V_1 to account for the differences in the body size within the study population, as the following; [32]

$$CL_i = TVCL \cdot \left(\frac{Wt_i}{Wt_{median}}\right)^{0.75} \tag{3}$$

$$V_i = TVV \cdot \left(\frac{Wt_i}{Wt_{median}}\right) \tag{4}$$

where CL_i and V_i are the individual values of CL and V_1 for individual i with body weight of Wt_i, Wt_{median} is the median body weight of the study population, TVCL and TVV are the typical values of CL and V_1 in the study population (i.e. 152 L/h and 6.3 L, respectively, Table 2).

Bacterial ETX release was linked to the bacterial elimination where a scaling factor (SF) was used to quantify the ETX release per bacterial CFU. ETX elimination was assumed to be nonlinear as reported previously by Thorsted *et al.* [16] according to;

$$\frac{d(ETX)}{dt} = \frac{CL}{V_1} \cdot SF \cdot B - \frac{V_{max}}{k_m + C_{ETX}} \cdot C_{ETX} \quad ; \; ETX_0 = 0 \tag{5}$$

where ETX is the ETX level in endotoxin unit (EU), SF is the ETX bacterial release scaling factor, V_{max} is the maximum ETX elimination rate, C_{ETX} is ETX concentration, k_m is ETX concentration at half of V_{max}, and ETX_0 is the baseline ETX.

Table 2
Final model parameter estimates.

Parameter (unit)	Description	Estimate (RSE%)	BSV in CV% (RSE %) [*Shrinkage*%]
E. coli-related parameters			
CL (L h^{-1})	bacterial clearance	152 (13%)	70 (14%) [9%]
V_1 (L)	volume of distribution for bacteria	6.3 (7%)	–
SF (EU CFU^{-1})	ETX bacterial release scaling factor	0.00008 (6%)	–
ETX - related parameters			
V_{max} (EU h^{-1})	the maximum ETX elimination rate	439,000 (1%)	–
k_m (EU L^{-1})	ETX concentration at half of V_{max}	13,400 (11%)	106 (19%) [28%]
V_2 (L)	volume of distribution for ETX	30.4 (11%)	140 (13%) [2%]
TNF -related parameters			
MTT_{TNF} (h)	mean transit time for TNF in plasma	1.31 (7%)	56 (12%) [51%]
E_{max1} (-)	the maximum stimulatory effect of ETX on TNF production rate	2680 (2%)	–
C_{50}(EU L^{-1})	initial ETX concentration producing half of the maximum effect on TNF	279 (2%)	–
E_{max2} (-)	the maximum stimulatory effect of ETX on C_{50} production rate	45,300 (1%)	–
TC_{50}(EU L^{-1})	the ETX concentration producing half of the maximum effect on C_{50} inducing tolerance	29,800 (1%)	–
γ(-)	sigmoidicity coefficient for Emax relationship	2.92 (3%)	–
MTT_{C50} (h)	Mean transit time for C_{50}	6.32 (2%)	–
$S_{0\,TNF}$ (ng L^{-1})*	TNF concentration at baseline	180	67 (26%) [26%]
IL-6 - related parameters			
$MTT_{IL\text{-}6}$ (h)	mean transit time for IL-6 in plasma	1.46 (6%)	79 (28%) [13%]
$E_{slp,TNF(-)}$	the slope for TNF increase of IL-6 production rate	1.04 (2%)	–
$E_{slp,ETX}$(L^{-1} EU	the slope for ETX increase of IL-6 production rate	0.011 (8%)	–
$S_{0\,IL-6}$(ng L^{-1})	IL-6 concentration at baseline	44.5 (18%)	111 (12%) [7%]
Residual unexplained variability in CV%			
$\sigma_{E.\ coli}$	proportional residual error of bacteria	66.5 (5%)	[11%]
σ_{ETX}	proportional residual error of ETX	96 (9%)	[16%]
σ_{TNF}	proportional residual error of TNF	70 (4%)	[14%]
σ_{IL-6}	proportional residual error of IL-6	30 (0.1%)	[15%]

BSV: between subject variability.
RSE: relative standard error.
* the value was fixed from the previous run for model stability issue.

3.1.2. Host response

The previously developed ETX-cytokines model by Thorsted *et al.* was linked to the here established *E. coli*-ETX model, using the parameters from Thorsted's model as informative priors. In the proposed model, the triggered release of pro-inflammatory cytokines by bacterial exposure is mediated by ETX. Testing a function for a stimulatory effect of bacteria on TNF production (on top of the ETX effect), did not

improve the model fit significantly (Δ OFV = − 0.403). The section below describes the ETX-cytokines relationships adapted from Thorsted's model.

TNF changes were driven by the ETX levels using a stimulatory sigmoidal E_{max} model;

$$\frac{d(TNF)}{dt} = R_{in,TNF}\cdot\left(1+\frac{E_{max1}\cdot C_{ETX}^{\gamma}}{C_{50}^{\gamma}+C_{ETX}^{\gamma}}\right) - k_{TNF}\cdot TNF \quad ; TNF_0 = S_{0TNF} \tag{6}$$

where TNF is the TNF concentration, $R_{in,TNF}$ is the zero-order production rate of TNF, E_{max1} is the maximum stimulatory effect of ETX on TNF production rate, C_{50} is the ETX concentration producing half of the maximum effect on TNF, γ is the sigmoidicity factor, k_{TNF} is the first-order elimination rate constant of TNF, and S_{0TNF} is TNF concentration at baseline.

$R_{in,TNF}$ and k_{TNF} were derived as the following;

$$R_{in,TNF} = S_{0TNF}\cdot k_{TNF} \tag{7}$$

$$k_{TNF} = \frac{1}{MTT_{TNF}} \tag{8}$$

where MTT_{TNF} is the mean transit time for TNF in plasma.

The host develops tolerance to ETX as a result of a decay in the potency of ETX to stimulate TNF. This was implemented in the model by allowing C_{50} to increase over time as a function of ETX levels using a stimulatory E_{max} model. This implementation was originally developed based on a wide range of ETX exposure profiles, which increases the likelihood of adequate predictions. A delay in tolerance development was captured by having two transit compartments;

$$\frac{d(C_{50(1)})}{dt} = R_{in,C_{50}}\cdot\left(1+\frac{E_{max2}\cdot C_{ETX}}{TC_{50}+C_{ETX}}\right) - k_{C_{50}}\cdot C_{50(1)} \quad ; C_{50(1)_0} = C_{50_0} \tag{9}$$

$$\frac{d(C_{50(2)})}{dt} = k_{C_{50}}\cdot C_{50(1)} - k_{C_{50}}\cdot C_{50(2)} \quad ; C_{50(2)_0} = C_{50_0} \tag{10}$$

$$\frac{d(C_{50})}{dt} = k_{C_{50}}\cdot C_{50(2)} - k_{C_{50}}\cdot C_{50} \quad ; C_{50(3)_0} = C_{50_0} \tag{11}$$

where $C_{50(n)}$ is the n^{th} transit compartment to describe the increase of C_{50} due to tolerance, $R_{in,C_{50}}$ is the zero-order input rate constant of C_{50}, E_{max2} the maximum stimulatory effect of ETX on C_{50} input rate, TC_{50} is the ETX concentration resulting in half of the maximum increase rate of C_{50}, $k_{C_{50}}$ is the first-order rate constant of transiting between the C_{50} compartments , C_{50_0} is the baseline C_{50}.

$R_{in,C_{50}}$, $k_{C_{50}}$ were derived as the following;

$$R_{in,C_{50}} = C_{50_0}\cdot k_{C_{50}} \tag{12}$$

$$k_{C_{50}} = \frac{3}{MTT_{C_{50}}} \tag{13}$$

where $MTT_{C_{50}}$ is the mean transit time for C_{50}.

For IL-6, both TNF and ETX were proposed to stimulate its production using a linear effect model through effect functions (EFF_{TNF}, EFF_{ETX}), as the following;

$$EFF_{TNF} = E_{slp,TNF}\cdot\left(\frac{TNF}{S_{0,\,TNF}} - 1\right) \tag{14}$$

$$EFF_{ETX} = E_{slp,ETX}\cdot C_{ETX} \tag{15}$$

where $E_{slp,TNF}$, $E_{slp,ETX}$ are the slopes for TNF and ETX increase of IL-6 production rate.

The delayed increase in IL-6 levels was described by four transit compartments;

$$\frac{d(IL\text{-}6_{(1)})}{dt} = R_{in,IL\text{-}6}\cdot(1+EFF_{TNF}+EFF_{ETX}) - k_{IL\text{-}6}\cdot IL\text{-}6_{(1)} \quad ; IL\text{-}6_{(1)_0} = S_{0IL\text{-}6} \tag{16}$$

$$\frac{d(IL\text{-}6_{(2)})}{dt} = k_{IL-6}\cdot IL\text{-}6_{(1)} - k_{IL-6}\cdot IL\text{-}6_{(2)} \quad ; IL\text{-}6_{(2)_0} = S_{0IL\text{-}6} \tag{17}$$

$$\frac{d(IL\text{-}6_{(3)})}{dt} = k_{IL\text{-}6}\cdot IL\text{-}6_{(2)} - k_{IL-6}\cdot IL\text{-}6_{(3)} \quad ; IL\text{-}6_{(3)_0} = S_{0IL\text{-}6} \tag{18}$$

$$\frac{d(IL\text{-}6_{(4)})}{dt} = k_{IL-6}\cdot IL\text{-}6_{(3)} - k_{IL-6}\cdot IL\text{-}6_{(4)} \quad ; IL\text{-}6_{(4)_0} = S_{0IL-6} \tag{19}$$

$$\frac{d(IL\text{-}6)}{dt} = k_{IL\text{-}6}\cdot IL\text{-}6_{(4)} - k_{IL\text{-}6}\cdot IL\text{-}6 \quad ; IL\text{-}6_{(5)_0} = S_{0IL\text{-}6} \tag{20}$$

where IL-6 is the concentration of IL-6, $R_{in,IL-6}$ is the zero-order production rate of IL-6, k_{IL-6} is the first-order rate constant for transiting between the different IL-6 transit compartments, S_{0IL-6} is the baseline concentration of IL-6.

$R_{in,IL-6}$, and k_{IL-6} were derived as the following;

$$R_{in,IL\text{-}6} = S_{0IL\text{-}6}\cdot k_{IL\text{-}6} \tag{21}$$

$$k_{IL-6} = \frac{5}{MTT_{IL-6}} \tag{22}$$

where $MTT_{IL\text{-}6}$ is the mean transit time for IL-6.

3.2. Modelling results and diagnostics

The final estimates of model parameters and the attached uncertainties are reported in Table 2. pcVPCs, and individual plots of model fits (Figs. 2, 3, and 2s) for the different DVs showed an overall good capacity of the model to describe the data. The peak levels of TNF and the terminal concentrations of ETX were somewhat less well predicted (being slightly underpredicted and overpredicted, respectively).

3.3. Model external evaluation

The TNF, and IL-6 profiles were simulated over four hours implementing the reported dose up-titration for the external data (Table 1). To account for the lower body size of the external data study population, allometric scaling based on the body weight was implemented using the following equation;

$$\theta_{newpop,\,scaled} = \theta_{ref}\cdot\left(\frac{Wt_{newpop,scaled}}{Wt_{ref}}\right)^{a} \tag{23}$$

where $\theta_{newpop,scaled}$ is the scaled parameter for the new population, θ_{ref} is the typical parameter estimate in the reference population used for the current model development, $Wt_{newpop,scaled}$ is the median body weight in the external data (fixed to the median of 15 kg due to lack of individual data), Wt_{ref} is the median body weight in the reference population, a is the allometric exponent which was set to 0.25 for physiological times, 0.75 for clearance processes, or 1 for body size parameters as reported in the literature [32–34]. Table 3 summarises the scaled parameters with the corresponding scaling exponent.

The simulations results are presented in Fig. 4 as overlay plots of the simulated model profiles and the literature data for TNF and IL-6. The plots showed an overall good description of the data which reflects the model's ability to capture the kinetics of cytokines under different

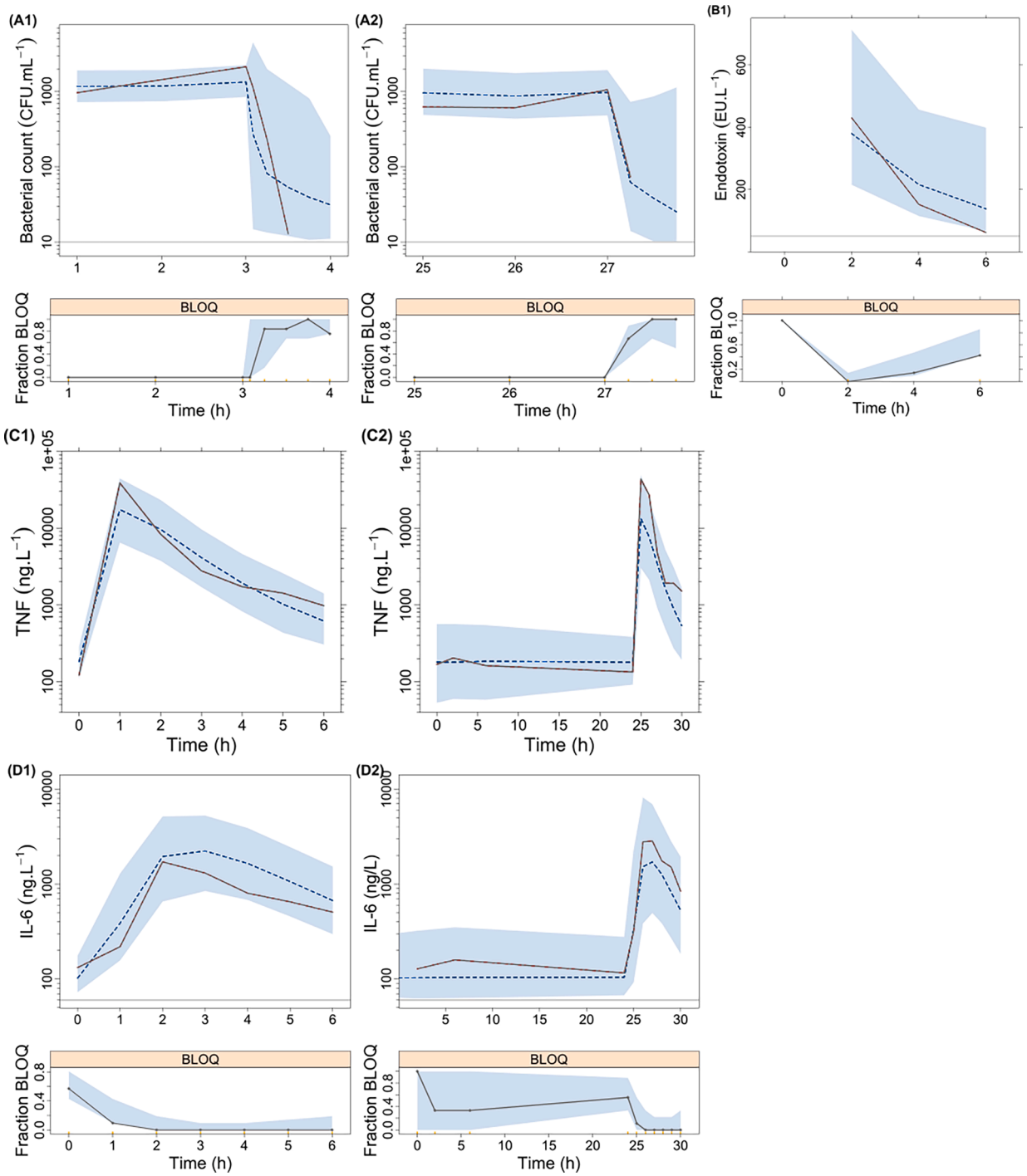

Fig. 2. Prediction corrected visual predictive checks of the different observed variables; panel (A); blood bacterial count, (B) Endotoxin, (C) TNF, (D) IL-6. The grey solid lines represent the median of the observed concentrations, and the blue dashed lines represent the median of simulated concentrations. The grey horizontal solid lines represent the lower limit of quantification. The shaded blue areas correspond to the 95% confidence interval for the simulated median. Panels (A), (C), and (D) have two subplots; 1 for data from studies (2, 3), and subplot 2 for study 1 with different time scales to account for observations preceded by a 24-h saline infusion (Table 1s). BLOQ; below the limit of quantification.

bacterial exposure scenarios.

3.4. Model simulations for different bacterial exposure scenarios

Model simulations revealed different cytokine profiles for the different exposure scenarios given the same total bacterial burden (Fig. 5). Exposure to the lowest initial bacterial load of 0.25 CFU × $10^8 h^{-1}$ (i.e. 5%, 15%, then 80% of the total bacterial dose per h) triggered the lowest cytokine release (in terms of C_{max} and AUC). The highest cytokine release was observed with exposure to the highest initial bacterial burden of 4 CFU × $10^8 h^{-1}$ (80%, 15%, then 5% of the total bacterial dose per h).

4. Discussion

In the current analysis, we present a mathematical modelling

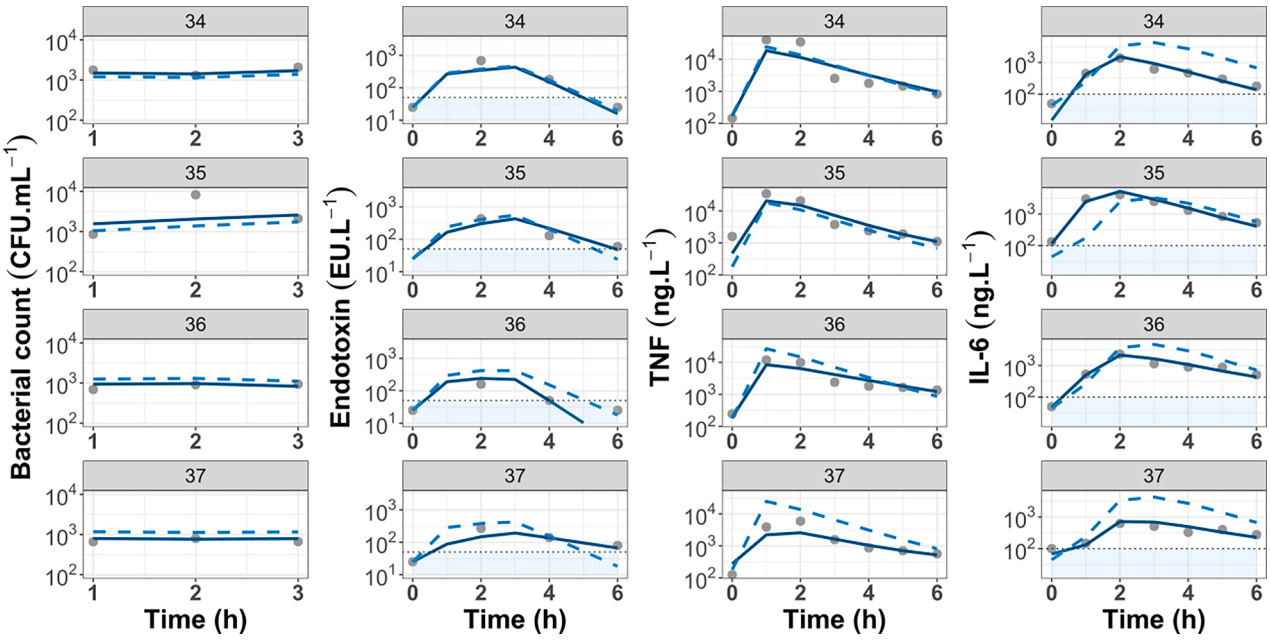

Fig. 3. Individual model fit for a sample of the study population (ID 34:37). The grey dots represent the observations, solid dark blue lines represent the individual model prediction (IPRED), dashed light blue lines represent the population model prediction (PRED), the dotted horizontal dotted black line represents the lower limit of quantification (LLOQ), while the blue bands used to highlight data below the limit of quantification (BLOQ). For ETX subplots, the observations, and model predictions at time point zero were BLOQ and were set to half of LLOQ for visualisation.

Table 3
Parameter scaling for external model evaluation.

Parameter	Description	Unit	Exponent	Scaled parameter
CL	bacterial clearance	L h^{-1}	0.75	101.8
V_1	volume of distribution for bacteria	L	1	3.7
$V_{max,ETX}$	the maximum ETX elimination rate	EU h^{-1}	0.75	294,004
V_2	volume of distribution for ETX	L	1	17.8
$MTT_{C_{50},TNF}$	mean transit time for $C_{50,TNF}$	h	0.25	5.6
MTT_{TNF}	mean transit time for TNF	h	0.25	1.14
MTT_{IL-6}	mean transit time for IL-6 in plasma	h	0.25	1.28

framework that characterises the cytokine kinetics triggered by exposure to intact live *E. coli* as observed in a porcine model of sepsis. The model quantitively captures the time courses of *E. coli* and the bacterial release of ETX, and predicts the kinetics of TNF, and IL-6. The model was applied to external literature data [28–30] from piglets receiving live *E. coli* infusions using a different experimental set-up. The model provided a good prediction of the cytokine kinetics for the external data. Moreover, the model was applied in simulations to explore cytokine kinetics at different bacterial exposure scenarios, exemplifying that it is not only the total bacterial burden that drives the host response, but also the rate of exposure. The similarity between pigs, and humans in terms of physiology and the components of innate immune response allows better chances for the translation of these results to clinical research [19,35].

The bacterial dynamics were characterised by a one-compartment model with linear elimination (Fig. 1). The current data did not support the estimation of any bacterial multiplication in the bloodstream. This is in line with the lack of detectable bacteria in the blood for most of the animals within 30 min after stopping the bacterial infusion (most of the observations were BLOQ). This result also aligns with a recent review [36] on the pathways of bacterial elimination from the bloodstream, that elaborated that free bacteria cannot proliferate in the

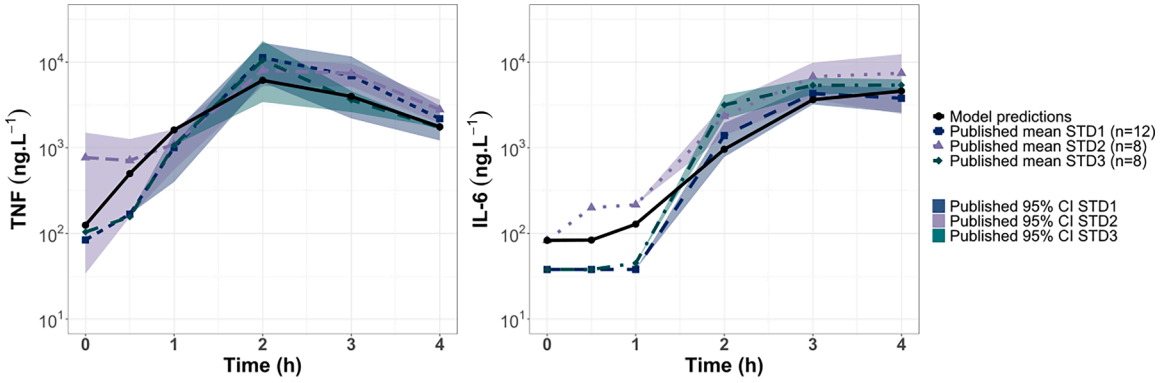

Fig. 4. Overlay plots of model predictions and external literature data. Solid black lines represent model predictions for a typical individual, and blue, green and violet lines with different point and line shapes represent the observed means from the different studies. The attached bands represent the published 95% confidence interval for the means.

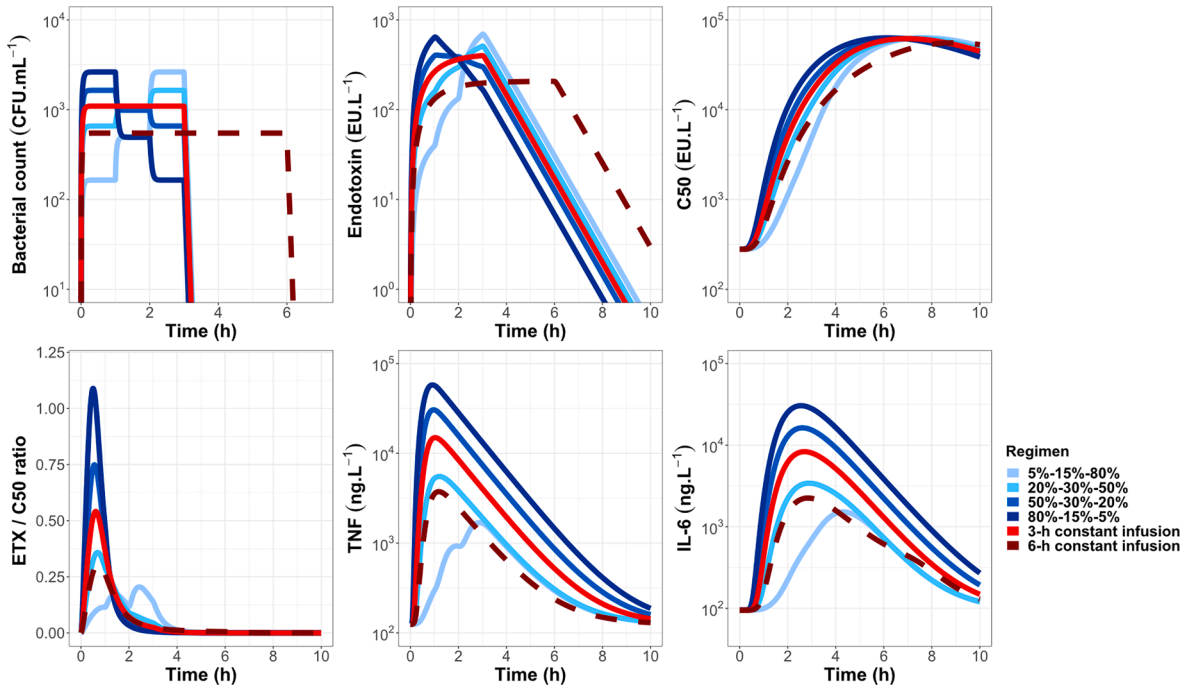

Fig. 5. Model predictions for the time course of blood bacterial count, endotoxin, tolerance (C_{50}), ETX/C_{50} ratio, TNF, and IL-6 under different simulated bacterial exposure scenarios with a total administered dose of 5×10^8 CFU. Red lines represent the constant bacterial infusion scenario for 3 h (solid red line) or 6 h (dashed dark red). Blue lines represent the 3-hour bacterial infusion changed every hour. Blue colour ranged from the darkest blue indicating the highest initial bacterial exposure to the lightest blue indicating the lowest initial bacterial exposure. The legend depicts the changing infusion dose as a percentage of the total dose.

bloodstream. Upon friction with the blood cells and vessel walls, the bacterial surface gains triboelectric charge which hinders the bacterial metabolic exchange needed for proliferation. The rapid bacterial elimination from the bloodstream may be attributed to bacterial killing at the erythrocyte surface by oxidation. The dead bacteria are then decomposed and digested in the liver and spleen [36]. In septic patients, the infection usually has a local infectious focus where the bacteria might have the capacity to replicate before they disseminate into the blood stream. Although the experimental design used here does not allow for such a replication rate to be estimated, the prediction of blood bacterial kinetics may be performed according to assumed input rates (Fig. 2 (A1, A2), 3).

The bacterial release of ETX is linked to the disruption of outer membrane of intact bacteria due to death, which could be mediated by the immune system [37]. This represents a crucial step in the activation of TLR-4 which in turn provokes a downstream cascade that ultimately leads to the release of inflammatory cytokines [38]. The bacterial elimination was here linked to ETX release by an estimated scaling factor (Fig. 1), which indicates the ETX release per bacterial CFU. ETX is considered a potent immunostimulant heavily involved in the pathogenesis and virulence of Gram-negative bacteria. Different experimental studies in rodents indicated the liver as the principal reticuloendothelial clearance site of ETX with less contributions from spleen, and kidneys [39–40]. The kinetics of ETX was described by a one-compartment model with saturable (non-linear) elimination. The wide sampling time interval (every 2 h) for ETX in the present data limited the possibility of capturing any early rapid phase of distribution.

Although endotoxemia is an often used experimental model, its ability to adequately reflect the complex and heterogenic condition of sepsis has been questioned [18–19]. Moreover, several adjunctive treatment agents (e.g. immunomodulators) that worked efficiently in the endotoxemia model, failed to show clinical efficacy when tested in septic patients [41–42]. This could be due to the use of ETX as the only PAMP triggering the host response, and lack of clear staging of sepsis severity in animal models [43]. However, also other factors might contribute to the failure of these clinical trials, for instance overlooking the variable ETX-liberating effect of the different antibiotics used and the timing of the antibiotic administrations [44–45]. To contribute to the understanding of the use of endotoxemia as a model for sepsis, we here explored whether the cytokine response would be different when triggered by intact bacteria rather than ETX exposure.

The model successfully described the cytokine kinetics without a need to update the ETX-cytokines model structure, and without major changes in parameter estimates. This aligns with the accumulating evidence that ETX is the main virulent factor driving the inflammatory response to Gram-negative bacteria [1,38,46–47]. It is worth to note that the potency of ETX as the primary driver of the inflammatory response, does not negate the inflammatory properties of other bacterial components. However, it has been shown previously that ETX produces similar haemodynamic and clinical changes as live *E. coli* in conscious pigs [48].

In the present model, the change in TNF production rate was driven by the ETX concentration–time course (Fig. 1). For most of the animals a peak concentration of TNF was observed one hour after starting the three-hour bacterial infusion (Fig. 2 (C1, C2), and 3). This was followed by a gradual decline towards the baseline regardless of the continuation of the bacterial infusion, indicating the predominance of the anti-inflammatory response. This declining pro-inflammatory component was characterised in the model as development of tolerance to ETX, implemented by allowing the ETX potency to decay with ETX exposure. For IL-6, the delay in the peak plasma concentration was described in the model by using a set of transit compartments with a mean delay time of 1.46 h (Fig. 2 (D1, D2), and 3). The stimulation of IL-6 production was driven by the time course of both ETX, and TNF with a higher stimulatory effect from TNF. Previously, results of human and animal studies demonstrated that TNF is an important stimulus to the induction of circulating IL-6 during sepsis [49–50]. The ETX contribution to the stimulation of IL-6 in the present model could be a surrogate to the impact other unmeasured mediators.

The role of ETX in invoking the pro-inflammatory cytokines, and

thus in the pathogenesis of sepsis, is supported by several studies on antibiotic-induced release of ETX [20,41,44–45]. In these studies, administration of antibiotics acting on the cell wall of Gram-negative bacteria, particularly penicillin-binding protein 3 inhibitors, led to a substantial increase of plasma ETX concentration and a profound inflammatory response [51]. In contrary, adding an anti-ETX agent in endotoxemia models, like polymyxin B which binds to ETX, has been linked to lower TNF levels and reduced mortality compared to untreated controls [41,52]. Several factors impact the antibiotic-induced release of ETX including the mechanism of action, the drug exposure profile, and the timing of receiving the antibiotic relative to sepsis progression. This highlights the importance of considering the impact of antibiotic-induced ETX release when testing the efficacy of new therapeutic agents [41].

The model described the cytokine kinetics in bacterial exposure scenarios beyond the one used for model development, as demonstrated when applied to external data (Fig. 4). The literature data were obtained in piglets receiving bacterial infusions of increasing amounts with a total dose of 16×10^8 CFU. This dose is about three times higher than the average bacterial dose in the data used for model development. Despite the discrepancies in the study designs, bacterial strains, and animal body sizes (summarised in Table 1), the model had the ability to adequately predict the cytokine kinetics. This shows the model to be able to predict cytokine kinetics in other experimental settings than those the original model was developed from, increasing its potential to translate to other scenarios.

Previous studies have experimentally explored different modes of bacteria or ETX administration, e.g. according to constant [53], increasing [54], or decreasing [55] infusion rates. This raised the interest to explore the sensitivity of the host response towards differences in the bacterial input rate given the same total bacterial load (here set to 5×10^8 CFU, i.e. same total dose used in the current data). Similar cytokine peak times were predicted across the different scenarios except for one scenario (i.e. 5%, 15%, then 80% scenario; the lightest blue) (Fig. 5). This discrepancy is related to the development of ETX tolerance. In cases with a high initial ETX-exposure, the tolerance is predicted to kick-in already before the ETX peak is obtained. The C_{50} then highly exceeds the ETX exposure by the end of bacterial infusion, and thus the stimulatory effect of the ETX on the TNF production is close to 0 by the time of 3 h (ETX/C_{50} ratio close to zero). On the contrary, with a low initial dose (the 5%, 15%, 80% scenario), the tolerance is less pronounced in the start, and the ETX exposure is still sufficiently high (ETX/C_{50} ratio) by the end of 3 h to stimulate the TNF production. However, the total TNF production will also be the lowest in this case, as the tolerance has already been initiated when the highest ETX exposure is reached. These results elaborate that it is not only the total bacterial burden that drives the host response, but also the bacterial exposure profile (i.e. the bacterial time course). The application of the model to this unobserved scenario highlights how the model could be used to explore "what-if" scenarios beyond the data used for model development.

In the present analysis, we investigated the kinetics of two pro-inflammatory cytokines as part of the host response to exposure to intact bacteria. Although no significant difference in the host response to *E. coli* exposure was noticed compared to ETX exposure, the results are limited to these two cytokines. The ETX disposition model could be updated upon availability of more intense samples of ETX with the potential to describe a two-compartment distribution profile. The modelling framework may be further expanded to include also other immune response components. In the current model, ETX tolerance was implemented by allowing the potency of ETX to stimulate TNF to be reduced as a function of ETX exposure. Anti-inflammatory cytokines may have a role in the observed tolerance development by opposing the inflammatory response.

The present model quantitively described and predicted the cytokine kinetics triggered by *E. coli* exposure using data from a porcine sepsis model. The model could be a starting point for future translational research on the immune response in sepsis by accounting for parameter differences among species using allometric scaling. Furthermore, it could layout the basis for potential mechanism-based models predicting other experimental scenarios than those the original model was developed from. Including data on the impact of antibiotics or other types of interventions on the model components would be most valuable to quantitively characterise the host-pathogen-drug interaction which could help optimise therapy in sepsis. The model could also be applied in drug development research on immunomodulators use in sepsis.

CRediT authorship contribution statement

Salma M. Bahnasawy: Methodology, Formal analysis, Data curation, Writing – original draft. **Paul Skorup:** Investigation, Writing – review & editing. **Katja Hanslin:** Investigation, Writing – review & editing. **Miklós Lipcsey:** Investigation, Writing – review & editing. **Lena E. Friberg:** Conceptualization, Supervision, Funding acquisition, Methodology, Resources, Writing – review & editing. **Elisabet I. Nielsen:** Conceptualization, Supervision, Funding acquisition, Methodology, Resources, Writing – review & editing.

Declaration of Competing Interest

The authors declare the following financial interests/personal relationships which may be considered as potential competing interests: [Salma M. Bahnasawy, Lena E. Friberg, Elisabet I. Nielsen reports financial support was provided by European Union. Salma M. Bahnasawy, Lena E. Friberg, Elisabet I. Nielsen reports financial support was provided by Swedish Research Council].

Data availability

Data will be made available on request.

Acknowledgements

The modelling framework was applied in NONMEM enabled by resources provided by the National Academic Infrastructure for Supercomputing in Sweden (NAISS) and the Swedish National Infrastructure for Computing (SNIC) at UPPMAX partially funded by the Swedish Research Council through grant agreement no. 2022-06725 and no. 2018-05973.

This project has received funding from the European Union's Horizon 2020 research and innovation program under the Marie Skłodowska-Curie grant agreement No 861323. Salma M. Bahnasawy is a member of TIPAT consortium (Training towards Innovative personalized Antibiotic Therapy), an Innovative Training Network for early-stage researchers.

Appendix A. Supplementary data

Supplementary data to this article can be found online at https://doi.org/10.1016/j.cyto.2023.156296.

References

[1] D. Heumann, T. Roger, Initial responses to endotoxins and Gram-negative bacteria, Clin. Chim. Acta 323 (2002) 59–72.
[2] P. Arina, M. Singer, Pathophysiology of sepsis, Current Opinion in Anesthesiology 34 (2021) 77–84.
[3] W. Schulte, J. Bernhagen, R. Bucala, Cytokines in sepsis: Potent immunoregulators and potential therapeutic targets—an updated view, Mediators Inflamm. 2013 (2013) e165974.
[4] J.A. Kempker, G.S. Martin, A global accounting of sepsis, Lancet 395 (2020) 168–170.

[5] K. Reinhart, R. Daniels, N. Kissoon, F.R. Machado, R.D. Schachter, S. Finfer, Recognizing sepsis as a global health priority — A WHO resolution, N. Engl. J. Med. 377 (2017) 414–417.
[6] C.E. Hack, L.A. Aarden, L.G. Thus, Role of cytokines in sepsis, in: F.J. Dixon (Ed.), Advances in Immunology, Academic Press, 1997, pp. 101–195.
[7] B.G. Chousterman, F.K. Swirski, G.F. Weber, Cytokine storm and sepsis disease pathogenesis, Semin Immunopathol 39 (2017) 517–528.
[8] R.S. Hotchkiss, G. Monneret, D. Payen, Sepsis-induced immunosuppression: from cellular dysfunctions to immunotherapy, Nat Rev Immunol 13 (2013) 862–874.
[9] K. Phe, E.L. Heil, V.H. Tam, Optimizing pharmacokinetics-pharmacodynamics of antimicrobial management in patients with sepsis: A review, J Infect Dis 222 (2020) S132–S141.
[10] F. Steinhagen, S.V. Schmidt, J.-C. Schewe, K. Peukert, D.M. Klinman, C. Bode, Immunotherapy in sepsis - brake or accelerate? Pharmacol. Ther. 208 (2020), 107476.
[11] A.M. Peters van Ton, M. Kox, W.F. Abdo, P. Pickkers, Precision Immunotherapy for Sepsis, Front. Immunol. (2018) 9.
[12] J. Cavaillon, M. Singer, T. Skirecki, Sepsis therapies: learning from 30 years of failure of translational research to propose new leads, EMBO Mol Med 12 (2020) e10128.
[13] F. Meurens, A. Summerfield, H. Nauwynck, L. Saif, V. Gerdts, The pig: a model for human infectious diseases, Trends Microbiol. 20 (2012) 50–57.
[14] J.K. Diep, T.A. Russo, G.G. Rao, Mechanism-Based Disease Progression Model Describing Host-Pathogen Interactions During the Pathogenesis of Acinetobacter baumannii Pneumonia, CPT: Pharmacometrics & Systems Pharmacology 7 (2018) 507–516.
[15] A. Thorsted, E. Tano, K. Kaivonen, J. Sjölin, L.E. Friberg, E.I. Nielsen, Extension of pharmacokinetic/pharmacodynamic time-kill studies to include lipopolysaccharide/endotoxin release from *escherichia coli* exposed to cefuroxime, Antimicrob. Agents Chemother. (2020) 64, https://doi.org/10.1128/AAC.02070-19.
[16] A. Thorsted, S. Bouchene, E. Tano, et al., A non-linear mixed effect model for innate immune response: In vivo kinetics of endotoxin and its induction of the cytokines tumor necrosis factor alpha and interleukin-6, PLoS One 14 (2019) e0211981.
[17] D.R. Mould, R.N. Upton, Basic concepts in population modeling, simulation, and model-based drug development, CPT Pharmacometrics Syst Pharmacol 1 (2012) e6.
[18] M.J. Schultz, T. van der Poll, Animal and human models for sepsis, Ann. Med. 34 (2002) 573–581.
[19] M.P. Fink, S.O. Heard, Laboratory models of sepsis and septic shock, J Surg Res 49 (1990) 186–196.
[20] L.F. Poli-de-Figueiredo, A.G. Garrido, N. Nakagawa, P. Sannomiya, Experimental models of sepsis and their clinical relevance, Shock 30 (2008) 53–59.
[21] H. Wyns, E. Plessers, P. De Backer, E. Meyer, S. Croubels, In vivo porcine lipopolysaccharide inflammation models to study immunomodulation of drugs, Vet. Immunol. Immunopathol. 166 (2015) 58–69.
[22] K. Hanslin, J. Sjölin, P. Skorup, et al., The impact of the systemic inflammatory response on hepatic bacterial elimination in experimental abdominal sepsis, Intensive Care Med Exp (2019) 7, https://doi.org/10.1186/s40635-019-0266-x.
[23] P. Skorup, L. Maudsdotter, M. Lipcsey, A. Larsson, J. Sjölin, Mode of bacterial killing affects the inflammatory response and associated organ dysfunctions in a porcine E. coli intensive care sepsis model, Crit. Care 24 (2020) 646.
[24] P. Skorup, L. Maudsdotter, E. Tano, et al., Dynamics of endotoxin, inflammatory variables, and organ dysfunction after treatment with antibiotics in an escherichia coli porcine intensive care sepsis model, Crit. Care Med. 46 (2018) e634.
[25] A.-H.-X.-P. Chan Kwong, E.A.M. Calvier, D. Fabre, F. Gattacceca, S. Khier, Prior information for population pharmacokinetic and pharmacokinetic/pharmacodynamic analysis: overview and guidance with a focus on the NONMEM PRIOR subroutine, J Pharmacokinet Pharmacodyn 47 (2020) 431–446.
[26] M. Bergstrand, A.C. Hooker, J.E. Wallin, M.O. Karlsson, Prediction-corrected visual predictive checks for diagnosing nonlinear mixed-effects models, AAPS J 13 (2011) 143–151.
[27] S.L. Beal, Ways to fit a PK model with some data below the quantification limit, J Pharmacokinet Pharmacodyn 28 (2001) 481–504.
[28] A. Barratt-Due, E.B. Thorgersen, K. Egge, et al., Combined inhibition of complement (C5) and CD14 markedly attenuates inflammation, thrombogenicity, and hemodynamic changes in porcine sepsis, J. Immunol. 191 (2013) 819–827.
[29] A. Barratt-Due, A. Sokolov, A. Gustavsen, et al., Polyvalent immunoglobulin significantly attenuated the formation of IL-1β in Escherichia coli-induced sepsis in pigs, Immunobiology 218 (2013) 683–689.
[30] E.B. Thorgersen, B.C. Hellerud, E.W. Nielsen, et al., CD14 inhibition efficiently attenuates early inflammatory and hemostatic responses in Escherichia coli sepsis in pigs, FASEB J. 24 (2010) 712–722.
[31] Rohatgi A. WebPlotDigitizer. 2021.https://automeris.io/WebPlotDigitizer.
[32] J. Mordenti, Man versus beast: Pharmacokinetic scaling in mammals, J. Pharm. Sci. 75 (1986) 1028–1040.
[33] D.E. Mager, S. Woo, W.J. Jusko, Scaling pharmacodynamics from in vitro and preclinical animal studies to humans, Drug Metab Pharmacokinet 24 (2009) 16–24.
[34] X. Chen, D.C. DuBois, R.R. Almon, W.J. Jusko, Characterization and interspecies scaling of rhTNF- α pharmacokinetics with minimal physiologically based pharmacokinetic Models, Drug Metab Dispos 45 (2017) 798–806.
[35] K.H. Mair, C. Sedlak, T. Käser, et al., The porcine innate immune system: An update, Dev. Comp. Immunol. 45 (2014) 321–343.
[36] H. Minasyan, Mechanisms and pathways for the clearance of bacteria from blood circulation in health and disease, Pathophysiology 23 (2016) 61–66.
[37] A.M. O'Hara, A.P. Moran, R. Würzner, A. Orren, Complement-mediated lipopolysaccharide release and outer membrane damage in Escherichia coli J5: requirement for C9, Immunology 102 (2001) 365–372.
[38] E.T. Rietschel, T. Kirikae, F.U. Schade, et al., Bacterial endotoxin: molecular relationships of structure to activity and function, FASEB J. 8 (1994) 217–225.
[39] M.A. Freudenberg, N. Freudenberg, C. Galanos, Time course of cellular distribution of endotoxin in liver, lungs and kidneys of rats, Br J Exp Pathol 63 (1982) 56–65.
[40] E.S. Fox, P. Thomas, S.A. Broitman, Hepatic mechanisms for clearance and detoxification of bacterial endotoxins, J. Nutr. Biochem. 1 (1990) 620–628.
[41] R.D. Piper, D.J. Cook, R.C. Bone, W.J. Sibbald, Introducing critical appraisal to studies of animal models investigating novel therapies in sepsis, Crit. Care Med. 24 (1996) 2059–2070.
[42] J.D. Baumgartner, T. Calandra, Treatment of sepsis: past and future avenues, Drugs 57 (1999) 127–132.
[43] J.A. Buras, B. Holzmann, M. Sitkovsky, Animal models of sepsis: setting the stage, Nat Rev Drug Discov 4 (2005) 854–865.
[44] P. Lepper, T. Held, E. Schneider, E. Bölke, H. Gerlach, M. Trautmann, Clinical implications of antibiotic-induced endotoxin release in septic shock, Intensive Care Med 28 (2002) 824–833.
[45] R. Nau, H. Eiffert, Minimizing the release of proinflammatory and toxic bacterial products within the host: A promising approach to improve outcome in life-threatening infections, FEMS Immunol. Med. Microbiol. 44 (2005) 1–16.
[46] S. Akira, S. Uematsu, O. Takeuchi, Pathogen recognition and innate immunity, Cell 124 (2006) 783–801.
[47] H. Minasyan, Sepsis: mechanisms of bacterial injury to the patient, Scand J Trauma Resusc Emerg Med 27 (2019) 19.
[48] E. Schrauwen, E. Cox, A. Houvenaghel, Escherichia coli sepsis and endotoxemia in conscious young pigs, Vet. Res. Commun. 12 (1988) 295–303.
[49] D.M. Jablons, J.J. Mulé, J.K. McIntosh, et al., IL-6/IFN-beta-2 as a circulating hormone. Induction by cytokine administration in humans, J Immunol 142 (1989) 1542–1547.
[50] P. Brouckaert, D.R. Spriggs, G. Demetri, D.W. Kufe, W. Fiers, Circulating interleukin 6 during a continuous infusion of tumor necrosis factor and interferon gamma, J. Exp. Med. 169 (1989) 2257–2262.
[51] A.S. Dofferhoff, J.H. Nijland, H.G. de Vries-Hospers, P.O. Mulder, J. Weits, V. J. Bom, Effects of different types and combinations of antimicrobial agents on endotoxin release from gram-negative bacteria: an in-vitro and in-vivo study, Scand J Infect Dis 23 (1991) 745–754.
[52] Y.M. Yao, H.M. Tian, Z.Y. Sheng, et al., Inhibitory effects of low-dose polymyxin B on hemorrhage-induced endotoxin/bacterial translocation and cytokine formation in rats, J Trauma 38 (1995) 924–930.
[53] V. Spyropoulos, A. Chalkias, G. Georgiou, et al., Initial immune response in escherichia coli, staphylococcus aureus, and candida albicans bacteremia, Inflammation 43 (2020) 179–190.
[54] A. Castellheim, E.B. Thorgersen, B.C. Hellerud, et al., New biomarkers in an acute model of live escherichia coli-induced sepsis in pigs, Scand. J. Immunol.. 68 (2008) 75–84.
[55] B. Eissner, K. Matz, A. Smorodchenko, A. Röschmann, v Specht BU., Chronic porcine two-hit model with hemorrhagic shock and Pseudomonas aeruginosa sepsis, Eur Surg Res 34 (2002) 61–67.